The "Coloring Problem" in Solids: How It Affects Structure, Composition and Properties

Gordon J. Miller

Department of Chemistry, Iowa State University
Ames, IA 50011-3111, USA
E-mail: gmiller@iastate.edu

Received October 14, 1997

Keywords: Quantum chemistry / Intermetallic compounds / Transition metal cluster compounds / Crystallography / Electronic structure

The "coloring problem," as applied to the field of solid state chemistry, addresses the issues of structural preference as well as the distribution of different elements within a given structure. Both the connectivity and arrangement of elements in a solid affect physical and chemical properties, so a clear understanding of the forces controlling how elements will arrange themselves in a solid state structure creates the ability to predict structure-composition-property relationships. There are two fundamental energetic contributions that influence how elements in a structure order: the site energy and the bond energy. This review examines how these two parts of the total electronic energy work together to influence the observed structures, compositions, and properties of intermetallics and transition metal cluster compounds.

The study of chemical compounds fundamentally involves elucidation of the relationships among composition, structure, and properties. From a historical perspective, there are two types of compounds: Daltonides and Berthollides. All molecular and many solid state compounds follow the law of definite proportions, which demands integral ratios for their compositions. Berthollides, on the other hand, are nonstoichiometric compounds, and occur only in condensed matter (solids and liquids).[1] Although there are no general rules governing stoichiometry, simple electron counting rules like the octet rule, the 18-electron rule, and Wade's rules provide guidance for stable compositions.[2] Electronic structure theory gives theoretical justification for these simple rules, but application of these quantum mechanical models requires a knowledge of structure, both actual and hypothetical. An additional bonus from the results of electronic structure calculations is the possibility, in principle, of extracting information on physical and chemical properties. Of course, the quantitative accuracy of these predictions depends on the level of approximation used in the quantum mechanical calculations. Such theoretical studies combined with an experimental program involving synthesis, careful structural characterization, and measurements of physical properties allow a thorough examination of the fundamental relationships among composition, structure, and properties. Certain extended solids, in particular intermetallics and transition metal cluster compounds, provide superb examples for systematic investigations of these relationships.

Structure-property relationships can already be witnessed with the main-group elements,[3] and are strongly coupled to valence electron concentration (*vec*), which equals the number of valence *s* and *p* electrons per main-group atom (for the transition elements, valence *s*, *p*, and *d* electrons are

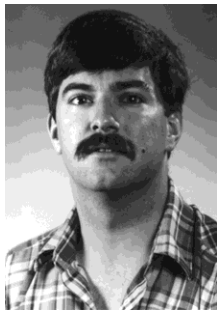

Gordon J. Miller was born in Utica, New York, USA. He received a B.S. degree in chemistry from the University of Rochester in 1982, and a Ph.D. in chemistry, under the supervision of Professor Jeremy K. Burdett, from the University of Chicago in 1986. He then began a postdoctoral research position in the group of Professor Arndt Simon at the Max-Planck-Institut für Festkörperforschung in 1987. In 1990, he joined the chemistry faculty at Iowa State University, where he is currently an Associate Professor. In 1995, he was awarded the Exxon Faculty Fellowship in Solid State Chemistry. His research group is studying structure-property relationships in extended solids, low temperature routes to new inorganic materials, and electronic structure theory of solids.

MICROREVIEWS: This feature introduces the readers to the authors' research through a concise overview of the selected topic. Reference to important work from others in the field is included.

  1434–1948/98/0505–0523 $ 17.50+.50/0

needed; for lanthanides and certainly the actinides, valence *f* electrons must be included as well). For main-group elements with *vec* less than four, closed packed (ccp, hcp or bcc) metallic structures form.[4] If *vec* is greater than or equal to four, open network, nonmetallic structures occur.[4] The inert electron-pair effect in sixth-period elements, e.g., Tl, Pb, Bi, and Po, creates exceptions to these trends.[5] A theoretical technique called second moment scaling of the electronic energy density of states provides a rationale for the observed structural trends of the elements.[6] Complete electronic structure calculations are required, however, to assess observed properties. For example, the observed decrease in electrical conductivity as pressure increases for elemental Ca, Sr, and Ba has been explained by the results of detailed band structure calculations.[7]

As composition becomes a variable, potential structural complexity increases dramatically with respect to both the network of interatomic connections as well as the exact arrangement of the different atoms throughout the structure. The second aspect is also called the *site preference* problem, which is a specific application of the more general *coloring* problem.[*] How atoms are distributed within a network can influence not only to what extent different atoms occur in a compound, i.e., stoichiometry, but also the nature of the electronic structure, i.e., physical and chemical properties. Moreover, there is a synergism between composition and geometrical structure which are blended via the electronic structure that leads to further chemical diversity. Intermetallic and transition metal cluster compounds are well suited for examining these fundamental problems of extended solids: subtle changes can be made in their compound compositions which allow detailed investigation of site preference. The Hume-Rothery intermetallic phases[9] provide exceptional examples for studying both structural complexities mentioned at the beginning of this paragraph: not only does structure change with *vec*, but the distribution of atoms among the different crystallographic sites in a given Hume-Rothery phase is closely related to its structure. Therefore, for multicomponent systems adopting extended structures the following questions arise: (1) for a given composition, what controls the observed structure; (2) in a given structure, how do the different chemical elements arrange themselves; (3) how does this arrangement of atoms influence the observed physical and chemical properties of a given compound; and (4) what is the fundamental relationship among structure, property, and composition for a particular chemical system?

Background

The coloring problem, better known as the "four-color problem" in mathematics, was one of the best known, unsolved mathematical challenges until it was solved in 1976.[10] It defied solution for over one hundred years (since 1852), while attracting the attention of nearly every mathematician in the late nineteenth and throughout the twentieth century. The original basic problem is "to find the smallest number of colors necessary to color the countries of any map so that each two countries with a common border have different colors."[**] This problem belongs to the discipline of *graph theory.*[12] A *graph* is a collection of points, called *vertices*, with various pairs of points joined by a collection of arcs, called *edges.* A vertex has *valence m* if exactly *m* edges meet at that vertex. A *map* is a graph in which each vertex has valence at least three, and with edges that form simple closed curves, called *faces.* The application of this problem to chemistry is clear: the structures of chemical compounds are often represented by graphs in which atoms occupy *vertices*, and bonds often correspond to *edges* in the graph. The chemist wonders, which coloring has the lowest energy? In these chemical examples, however, "coloring" occurs at the vertices, and not at the faces.[***] the idea of reciprocity is important for justifying the equivalence of these two mathematical problems.[10]

The coloring problem occurs in some classic molecular examples: the simplest case being linear triatomic molecules. Both CO_2 and N_2O are linear molecules, but only CO_2 has inversion symmetry. The explanation for the arrangements OCO or NNO and not OOC or NON is simply that 16-electron triatomic molecules require the more electronegative component to occupy the terminal position, i.e., the site with lower coordination number.[14] This effect also occurs in the cage structures of S_4N_4 and As_4S_4,[15] (see Figure 1) which adopt identical molecular topologies: one site is two-bonded (N in S_4N_4; S in As_4S_4), the other is three-bonded (S in S_4N_4; As in As_4S_4). Since the Pauling electronegativities for these three elements increase from As to S to N, the arrangement of atoms in these molecules has the more electronegative element at the two-bonded position.

Figure 1. Molecular structures of As_4S_4 (left) and S_4N_4 (right); white circles are S atoms, black circles are As or N atoms

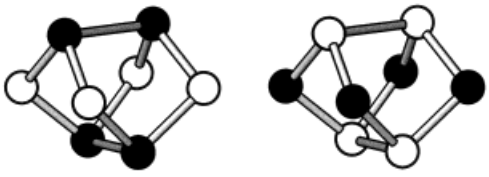

As_4S_4 S_4N_4

Molecular orbital theory can substantiate this conclusion through the principle of *topological charge stabilization.*[16] When a Mulliken population analysis[17] is applied to the

[*] A succinct statement of the coloring problem in chemical systems is, "Given a molecular or extended network and several different types of atoms or chemical groups, what is the best way to distribute them in the network for a fixed stoichiometry?"[8]

[**] The German mathematician Möbius is credited with its origination in the form of a puzzle to his students.[11]

[***] In terms of graph theory, another statement of the coloring problem is, "Consider a fixed molecule or solid state framework which is then populated with different sorts of atoms or atom groupings. Such a mapping of vertices to atoms is called a coloring, and the different atoms or units are associated with different colors."[13]

results of a molecular orbital calculation on a *homonuclear* molecular structure, differences in atomic populations, i.e., the number of valence electrons assigned to an atomic site in the molecule, usually occur. For an isostructural *heteronuclear* molecule, the most electronegative element will occupy the site with the largest Mulliken population. The simple Hückel theory can verify this conclusion. Consider a molecule composed of atoms, which are each described by a set of valence atomic orbitals $\{\chi_i\}$ with atomic orbital energies α_i ($\alpha_i < 0$). The strengths of the atomic orbital interactions in the molecule are prescribed by a set of resonance integrals β_{ij} ($\beta_{ij} < 0$). In the LCAO approximation, a molecular orbital is expressed as

$$\psi_n = \Sigma_i \, c_{ni} \, \chi_i \tag{1}$$

where c_{ni} is the numerical coefficient of the i^{th} atomic orbital in the n^{th} molecular orbital and the summation covers all valence atomic orbitals $\{\chi_i\}$ in the molecule. The energy of this molecular orbital can then be written as

$$E_n = \Sigma_i \, c_{ni}^2 \alpha_i + \Sigma_i \, \Sigma_{j \neq i} \, c_{ni} c_{ij} \beta_{ij} \tag{2}$$

The total valence electron energy, E_{mo}, is the sum of the molecular orbital energies E_n times their corresponding occupation numbers ($z_n = 0$, 1, or 2), which gives the result[18]

$$\begin{aligned} E_{\text{mo}} &= \Sigma_n \, z_n \, E_n = \Sigma_n \, z_n \, (\Sigma_i \, c_{ni}^2 \, \alpha_i + \Sigma_i \, \Sigma_{j \neq i} \, c_{ni} \, c_{nj} \, \beta_{ij}) \\ &= \Sigma_i \, (\Sigma_n \, z_n \, c_{ni}^2 \,) \, \alpha_i + \Sigma_i \, \Sigma_{j \neq i} \, (\Sigma_n \, z_n \, c_{ni} \, c_{nj}) \, \beta_{ij} \\ E_{\text{mo}} &= \Sigma_i \, q_i \, \alpha_i + \Sigma_i \, \Sigma_{j \neq i} \, p_{ij} \, \beta_{ij} \end{aligned} \tag{3}$$

where q_i is the atomic orbital population (Mulliken population in Hückel theory) and p_{ij} is the overlap population[17] (Coulson bond order index[19]) which are defined by the equations

$$q_i = \Sigma_n \, z_n \, c_{ni}^2 \tag{4}$$

$$p_{ij} = \Sigma_n \, z_n \, c_{ni} \, c_{nj} \tag{5}$$

The principle of topological charge stabilization uses just the first term of equation (3), i.e., the most stable coloring of a heteronuclear molecule is the one for which the most electronegative element, i.e., the one with the lowest α_i's, occupies the site with the greatest Mulliken population, q_i, in the *homonuclear* model of the molecule.

Figure 2. Simple representation of three-center four-electron bonding; in the trigonal bipyramidal molecule PF_4CH_3, the methyl group occupies the equatorial position; the linear F−P−F fragment along the axial direction involves three-center four-electron bonding, whose simple molecular orbital picture is shown; the nonbonding orbital has a node at the P atom, which results in the axial sites being generally preferred by the most electronegative ligands

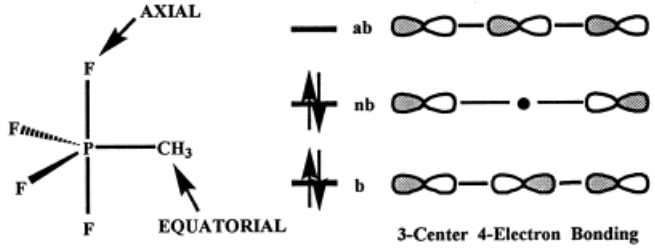

Additional examples of the application of this principle include five-coordinate main group molecules (see Figure 2), which adopt either trigonal bipyramidal or square pyramidal structures.[20] Both arrangements have two inequivalent sets of ligands, labeled axial and equatorial, which immediately lead to a site preference problem. In ten-electron trigonal bipyramidal molecules, e.g., PCl_3F_2 and $PF_4(CH_3)$,[2] the more electronegative F atoms prefer the axial sites, although these molecules undergo rapid pseudorotation. In each case, the more electronegative ligand is involved in three-center four-electron bonding along three collinear atoms.[21] The four electrons in this simple model occupy one bonding and one nonbonding molecular orbital (see Figure 2). The bonding orbital is delocalized throughout the three atomic orbitals, while the nonbonding molecular orbital has only ligand character, which provides the electronic driving force for the observed substitution pattern. Ligands in the equatorial sites of these molecules are involved in two-center two-electron bonding with the central atom. On the other hand, twelve-electron square pyramidal molecules like $XeOF_4$ have the more electronegative ligands (F atoms in $XeOF_4$) in the equatorial sites, which involve two three-center four-electron interactions.

When nonorthogonal atomic orbital basis sets are used in electronic structure calculations, as in the extended Hückel theory,[22] the expression for the total valence electron energy E_{mo} becomes slightly modified from equation (3). The overlap integrals S_{ij} are now explicitly included during calculation of the electronic energy levels, and expressions for the Mulliken population and overlap population become

$$q_i = \Sigma_n \, z_n \, (\, c_{ni}^2 + c_{ni} \, c_{nj} \, S_{ij}) \tag{6}$$

$$p_{ij} = \Sigma_n \, 2 \, z_n \, c_{ni} \, c_{nj} \, S_{ij} \tag{7}$$

Then, after some simple algebraic manipulations of the molecular orbital energy values, the total valence electron energy is

$$E_{\text{mo}} = \Sigma_i \, q_i \, \alpha_i + \Sigma_i \, \Sigma_{j \neq i} \, p_{ij} \, (\beta_{ij} - S_{ij} \, \alpha_i) \tag{8}$$

The first term in expressions (3) or (8) can be interpreted as the energy contribution from the valence electron configurations of the different atoms or ions in the structure, which is the *site energy*. The value of this term is sensitive to the degree of charge transfer between atoms as well as the coordination geometry at each site. The second term is a net two-center interaction term, the *bond energy*, and will be minimized when only bonding and nonbonding orbitals are occupied by providing maximum overlap populations p_{ij}.

This type of transformation of the total valence electron energy does not require a knowledge of the eigenstates of the system, i.e., $\{\psi_n\}$, provided another method can calculate the population terms, q_i and p_{ij}.[23] These chemical quantities are the matrix elements of the density matrix,[*]

[*] The density matrix elements are expansion coefficients of the total charge density in the atomic orbital basis set. Diagonal elements are the charge densities to associate with each orbital in the system; off-diagonal elements are bond orders between two different atomic orbitals on different atoms.

which can be determined without knowing the eigenstates by using, for example, the recursion method.[24] Furthermore, expressions (3) and (8) are general for all types of chemical systems: molecules, crystalline solids, amorphous solids, liquids, quasicrystalline solids, and defective crystalline materials. For solids, E_{band} replaces the symbol E_{mo} to describe the total valence electron energy from the occupation of energy bands rather than molecular orbitals. In subsequent discussions, we shall call this energy the total orbital energy, E_{orb}. This transformation of the total energy introduces a much more chemical approach to the analysis of electronic structure of solids. Furthermore, with respect to the "coloring" problem in chemical structures, the tight-binding expressions in equations (3) and (8) point to two contributions: atoms arrange themselves to provide the lowest site energy and to minimize the bond energy.

Figure 3. Structure of the quasi-infinite $^{1}_{\infty}[SnTe_5]^{2-}$ chain in K_2SnTe_5 and Tl_2SnTe_5;[25] white circles are Te atoms, black circles are Sn atoms

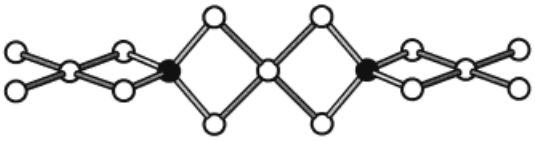

Consider one simple example of this problem: the quasi-infinite chain $^{\infty}_{1}[SbTe_5]^{2-}$ found in K_2SnTe_5 and Tl_2SnTe_5 (see Figure 3).[25] As the figure shows, this chain consists of tetrahedrally coordinated Sn atoms alternating with square planar coordinated, albeit slightly distorted, Te atoms, which we can formulate as $^{\infty}_{1}[(SnTe_{4/2})(TeTe_{4/2})]^{2-}$. X-ray diffraction studies are unable to differentiate between Sn ($Z = 50$) and Te ($Z = 52$) for these two sites, but their distribution has been inferred from the known crystal chemistry of these two elements. An extended Hückel calculation performed on a homonuclear chain (using only Te atomic orbital parameters) indicates that the more electropositive element [Sn; lower q_i's in equation (8)] would occupy the tetrahedrally coordinated site, and the more electronegative element [Te; higher q_i's in equation (8)] would occupy the site with square planar coordination. A direct comparison of the two different patterns shows the observed combination to be energetically preferred over the alternative by approximately 10.0 eV per formula unit if only nearest neighbor (four Sn−Te and four Te−Te) interactions are considered. Of this 10.0 eV energy difference, 1.2 eV is attributed to the difference in site energies and 8.8 eV is the difference in bond energies. The dominance of the bond energy difference reflects tetrahedral vs. square planar coordination at the two different sites. When second nearest neighbor interactions are included (Sn···Te along the chain in the tight-binding calculation), this total energy difference increases to 14.4 eV, of which 12.1 eV is due now to a difference in site energies, and 2.3 eV to a difference in bond energies. The dramatic change in how the two components contribute to the total energy arises from a significant difference in the coordination environment: Sn is surrounded by 4 + 2 Te atoms, whereas Te is coordinated by four Te atoms and two Sn atoms. Regardless, the Sn occupies the tetrahedral sites and Te, the square planar sites.

In extended solids the site preference problem has already been well documented for the spinels, $A^{2+}B_2{}^{3+}O_4$.[26] In these oxides, one-half the octahedral holes and one-eighth the tetrahedral holes are occupied by metal ions in the cubic closest packed oxide framework. A *normal* spinel would be $A_{(tet)}{}^{2+}B_{(oct)2}{}^{3+}O_4$, as in $Co_3O_4 \equiv Co_{(tet)}{}^{2+}Co_{(oct)}2^{3+}O_4$, whereas an *inverse* spinel would be $B_{(tet)}{}^{3+}$-$(A_{(oct)}{}^{2+}B_{(oct)}{}^{3+})O_4$, as in $CoFe_2O_4 \equiv Fe_{(tet)}{}^{3+}$-$(Co_{(oct)}{}^{2+}Fe_{(oct)}{}^{3+})O_4$. The crystal field theory achieved success by comparing the energies of octahedral and tetrahedral fields for different d^n electronic configurations. Strong preference for octahedral coordination occurs for d^1-d^4 and d^6-d^9 ions, which has been used to rationalize the different ionic arrangements in spinels. Of course, ligand field theory can also be applied to these examples with identical results.[2]

Perhaps a better example of the "coloring" problem is how to color the body-centered cubic (bcc) lattice with two different atoms at equal concentrations, i.e., AB. The cubic CsCl structure (Figure 4) is the alternant variant, with each A atom surrounded by eight nearest neighbor B atoms and six next nearest neighbor A atoms at a 15% larger distance. On the other hand, the CuTi structure (Figure 4) is a tetragonal modification of the bcc arrangement with alternating pairs of (001) planes of atoms. In CuTi, each A atom is coordinated by four A and four B nearest neighbors as well as four A and two B next nearest neighbors; each B atom is surrounded by four A and four B nearest neighbors and four B plus two A next nearest neighbors. In these two examples, the observed coloring depends on the *vec*, as also shown in Figure 4 for binary alloys of the transition metals.[27] Another possible coloring of this lattice is the NaTl structure (Figure 4),[28] which is limited to binary compounds of the pre- and post-transition elements. For the NaTl structure, there are four A and four B nearest neighbors plus six next nearest neighbor B atoms around each A atom. For this problem, semi-empirical calculations nicely reproduce the observed trend in structure.[27]

Therefore, with respect to these examples, the site preference problem is a specific corollary of the more general "coloring" problem. Extended solids offer the additional problem of disorder, which further complicates the problem. A general understanding (i.e., predictive algorithm) remains to be determined to elucidate solutions for the general case, but the following section examines a small number of examples from our research group to help build a body of data for the "coloring" problem in solids.

Applications

The remainder of this article focuses on specific examples of the "coloring problem" in extended solids from our group's research. The fundamental questions concern how structure, composition, and properties of extended solids are affected by the arrangement of different elements in a compound. Since intermetallic and transition metal cluster compounds are involved, these investigations reveal how

Figure 4. Structures of different AB colorings of the bcc lattice: (very top) CsCl structure; (center top) CuTi structure; (center bottom) NaTl structure; (very bottom) computed energy differences between the CsCl and CuTi arrangements vs. the average number of $s + d$ electrons; CsCl is the reference structure; the more stable structure has the lower value of ΔE for a given number of $s + d$ electrons; experimentally observed values are shown on the diagram

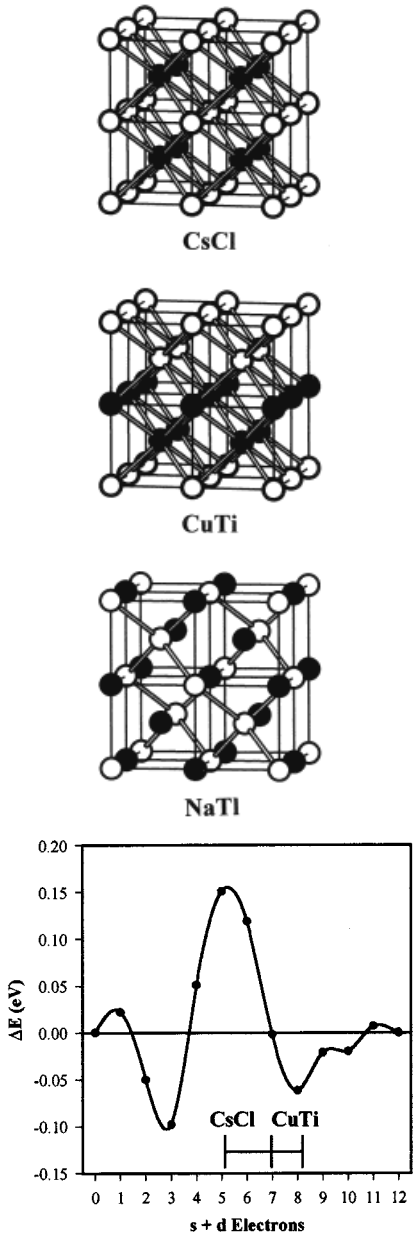

experiment and theory can work symbiotically to pursue some fundamental chemical questions. These applications are organized as follows: (1) kinetically vs. thermodynamically stable structures; (2) structural influences for a single composition but variable electron count; (3) site preferences and composition influenced by nearest neighbor interactions; (4) structure-composition relationships in intermetallics; and (5) composition-property effects.

Figure 5. Structures of the low and high temperature forms of Nb_3SI_7: (top) *o*-Nb_3SI_7; (bottom) *h*-Nb_3SI_7; black circles are Nb atoms, gray circles are S atoms, white circles are I atoms; figures on the left illustrate the two-dimensional layers of clusters, and those on the right show the local environments of the Nb_3 triangles; the point symmetry of the cluster in *o*-Nb_3SI_7 is C_s while in *h*-Nb_3SI_7 it is C_{3v}

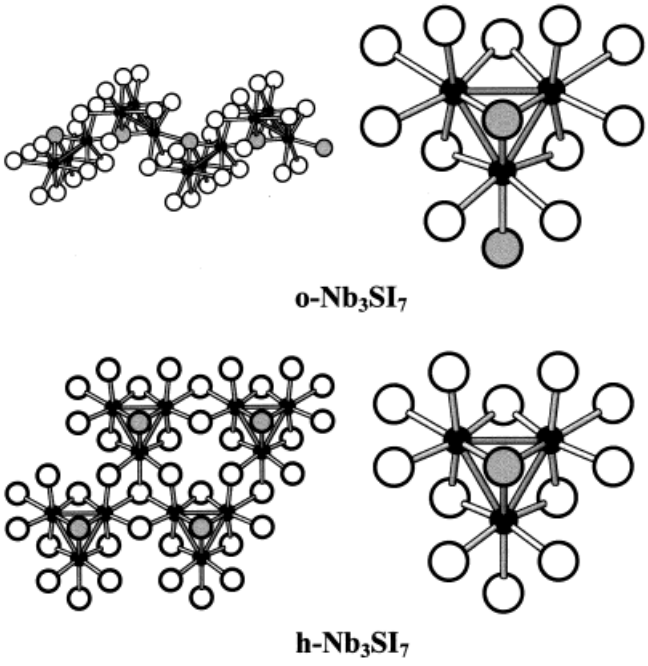

1. Kinetic versus Thermodynamic Products: Nb_3SI_7

The formation of solid state compounds is certainly controlled by both thermodynamic and kinetic factors. With temperature and pressure as fundamental variables, the complete study of a particular system involves numerous synthetic attempts under different conditions. Recent investigations with ternary transition metal/chalcogen/halogen systems containing metal clusters have uncovered a diverse collection of new layered compounds with various structures and properties.[29] One poignant example is Nb_3SI_7, which has been characterized in three topologically different layered structures (polymorphs, not polytypes!) depending upon the temperatures chosen for synthesis. All three structures, however, contain triangular Nb_3 clusters with capping sulfur atoms. Their differences arise in how these units are linked together. The coloring problem in this system addresses how sulfur and iodine form the anion matrix that contains the Nb_3 clusters.

At temperatures between ca. 300 °C and 650 °C, elemental niobium, sulfur, and iodine react in the molar ratio 3.0:1.0:3.5 to give a crystalline orthorhombic phase, *o*-Nb_3SI_7, whose structural formula is $Nb_3S_{1/2}{}^{i-a}I_3{}^{i}I_{6/2}{}^{a-a}$-$(I_{2/2}{}^{a-a}S_{1/2}{}^{a-i})$.[*] As seen in Figure 5, the Nb_3 triangle is capped by a single sulfur atom (S^i), and each edge is

[*] The notation for transition metal clusters differentiates between ligands bridging edges or faces of a cluster, i.e., X^i (i = *innen* = inner) and those connecting or terminating clusters, X^a (a = *aussen* = outer).[30]

bridged by an iodine atom (I^i). These $[Nb_3(\mu_3\text{-}S)(\mu_2\text{-}I)_3$ units are then connected together by six iodine atoms (I^{a-a}) linking two clusters and three ligands *trans* to the capping sulfur atom (two are I^{a-a} and one is S^{a-i}) linking three clusters. There is just one crystallographic type of sulfur atom in *o*-Nb_3SI_7: it caps an Nb_3 triangle, but it also bonds to an adjacent cluster (thus the S^{i-a} and S^{a-i} designations in the structural formula). In *o*-Nb_3SI_7 sulfur is 3+1 coordinated to Nb in a *cis*-divacant octahedral geometry. This local coordination structure at one of the anions gives rise to the undulating layered structure of *o*-Nb_3SI_7.

Figure 6. Schematic diagrams of the relationships in atomic orbital energies for three different elemental components of ternary compounds; the higher the electronegativity of an element, $\chi(X)$, the lower its valence orbital energies; for these schemes, $\chi(A) < \chi(B)$, so $E(A)'s > E(B)'s$; the interesting chemistry arises by considering how A and B relate to the third component C; (a) $\chi(A) < \chi(B) < \chi(C)$, (b) $\chi(A) < \chi(C) < \chi(B)$, (c) $\chi(C) < \chi(A) < \chi(B)$; electron transfer takes place until a constant electrochemical potential exists throughout the structure

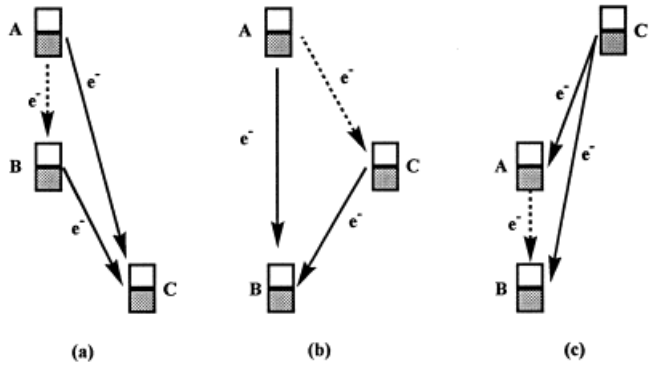

Above ca. 650°C, these elements form a layered hexagonal structure, *h*-Nb_3SI_7,[29] (see Figure 4) whose layers are related to those found in β-Nb_3I_8.[31] The corresponding structural formula for this compound is $Nb_3S_1{}^iI_3{}^iI_{6/2}{}^{a-a}I_{3/3}{}^{a-a}$. Each sulfur atom is just three-coordinated to Nb, and the layers are flat. The structures of *o*-Nb_3SI_7 and *h*-Nb_3SI_7 can be compared by examining the two different packing arrangements of anions: *o*-Nb_3SI_7 involves cubic closest packed anions $(\cdots c\cdots)$[32] with each (111) plane containing 1/8 sulfur and 7/8 iodine, while *h*-Nb_3SI_7 contains an alternating mixture of cubic closest packed and hexagonally closest packed layers $(\cdots hc\cdots)$[32] with sulfur occurring in alternate close packed layers to an extent 1/4 sulfur and 3/4 iodine. In *o*-Nb_3SI_7 the stacking arrangement of one anion "(111)" sheet (i.e., "SI_7") with respect to its two neighboring layers maximizes the S···S internuclear separation, or minimizes the electrostatic repulsion between neighboring sulfide ions. In both close packed anion arrays, Nb atoms occupy 3/8 of the total number of octahedral holes and are located close to the sulfur atoms. A combination of lattice energy[33] and extended Hückel[22] calculations on various models indicates that Nb−Nb bonding is optimized in *h*-Nb_3SI_7, but that the Madelung energy is lower for *o*-Nb_3SI_7. Quenching and annealing experiments conducted at different temperatures show that *o*-Nb_3SI_7 transforms to *h*-Nb_3SI_7 irreversibly at temperatures above ca. 650°C.

Thus, the coloring of the anion network in Nb_3SI_7 strongly influences the resultant total structure of the extended solid involving transition metal clusters. Ionic and covalent forces compete for the formation of a given atomic arrangement. At low temperatures, long range electrostatic interactions guide the formation of the kinetically stable *o*-Nb_3SI_7 by maximizing the separation between sulfide ions. At higher temperatures, however, the atoms rearrange to give a structure with lower internal energy, *h*-Nb_3SI_7, which retains certain structural features, e.g., the Nb_3 triangular cluster.[*]

The ternary niobium/sulfur/iodine system offers a further application of the coloring problem that is only possible in extended solids-nonstoichiometry. $Nb_3S_{1-x}I_{7+x}$ can be prepared from the elements for $x \leq 1$.[29][35] X-ray and neutron diffraction studies on polycrystalline powders and single crystals show that these layered compounds have structures related to β-Nb_3I_8 for $x > 0.6$ and *h*-Nb_3SI_7 for $x < 0.4$. A two-phase mixture of these structures exists for $0.4 < x < 0.6$. Throughout the series, moreover, sulfur and iodine atoms randomly occupy the anion site capping the Nb_3 cluster. Neutron powder diffraction on the compounds β-Nb_3I_8, $Nb_3S_{0.34}I_{7.66}$, and $Nb_3S_{0.64}I_{7.36}$ between 15 K and 300 K did not exhibit any ordering phenomena, i.e., no superstructure reflections nor any symmetry-lowering phase transitions. Magnetic susceptibility measurements give one unpaired electron per μ_3-I capped Nb_3 cluster, except in β-Nb_3I_8. We can understand the lack of superstructure from the electronic structures of μ_3-S capped Nb_3 groups and μ_3-I capped Nb_3 groups in the iodide matrix. Electronic and matrix effects work against each other to produce disorder: the six-electron Nb_3 cluster in Nb_3SI_7 has weaker Nb−Nb bonding but a smaller capping anion (sulfide) than the seven-electron cluster in β-Nb_3I_8. Thus, Nb−Nb distances remain nearly unchanged throughout the series $Nb_3S_{1-x}I_{7+x}$ and the Fermi levels do not vary with the composition variable *x*.

2. Coloring and Structure in Ternary MM′X Intermetallics

Intermetallic compounds adopt structures that are dependent, in part, on the number of valence electrons per formula unit. An understanding of this relationship between structure and electron count requires knowledge of the electronic structures and a good estimation of the structural energy differences for different arrangements of atoms. *Second moment scaling*[6] techniques and the *structural energy difference theorem*[4] have contributed greatly to the recent success of electronic structure calculations for sorting numerous binary intermetallic compounds. The second moment μ_2 for a quasi-continuous distribution of electronic states $\rho(E)$ (as one finds in an extended solid) is defined by the integral

$$\mu_2 = \int_{-\infty}^{\infty} E^2\rho(E)\mathrm{d}E \qquad (9)$$

[*] A new modification, *m*-Nb_3SI_7, has been recently characterized at temperatures exceeding 1000°C, but was first identified in the compound $Nb_7S_2I_{19} = [Nb_3SI_7]_2(NbI_5)$.[34]

Within the tight-binding (LCAO) approximation, this integral expression can be rewritten into a summation

$$\mu_2 = \Sigma_{i=1}^{N} \alpha_i^2 + \Sigma_{i<j} \beta_{ij}^2 \quad (10)$$

N is the number of atomic orbitals in the unit cell, α_i is the atomic orbital energy for the i^{th} atomic orbital, and β_{ij} is the resonance integral between different atomic orbitals i and j. For identical compositions, the first term in equation (10) is the same for all structural models. Second moment scaling, therefore, demands that for all structure types to be compared the unit cell and atomic positional parameters be selected to create equal second terms, $\Sigma_{i<j}\beta_{ij}^2$, and therefore equal μ_2 values. The structural energy difference theorem states that the energy difference between two structures is given to first order by the difference in the bonding contributions to the total energy, i.e., ΔE_{bond}. The total binding energy for a structure is generally the sum of a repulsive term, E_{rep}, and the bonding contribution, E_{bond}. E_{bond} can result from a Madelung (E_{mad}), molecular orbital or band structure (E_{orb}) calculation, while the repulsive term is a combination of short-range electrostatic and Pauli repulsion contributions, which are specifically proportional to coordination numbers. Heine has demonstrated that the second moment μ_2 is proportional to the average coordination number in a given structure.[36] Therefore, performing second moment scaling on various structural models creates equal E_{rep} terms in the total binding energy, and validates the structural energy theorem.[4]

Once the electronic structure calculations are completed, equation (3) or (8) can be used to provide a rationale, in chemical terms, for the predicted sorting diagram: an element will tend to adopt a single type of site that minimizes its site energy and bond energies. For a study of structural changes with valence electron concentration, the site energy changes rapidly with electron count due to the quadratic dependence of atomic orbital energies on charge. The relative electronegativities (χ) of the components in ternary A_x-B_yC systems give rise to three scenarios: (1) $\chi(C) > \chi(B) > \chi(A)$, (2) $\chi(B) > \chi(C) > \chi(A)$, and (3) $\chi(B) > \chi(A) > \chi(C)$. Figure 6 illustrates how electron transfer will take place as these elements form chemical bonds (the greater electronegativity implies lower atomic orbital energies). The sites ultimately selected by elements A and B in the C matrix will follow the ramifications of equation (8): lowest *site* and *bond* energies, which are governed by the extent of electron transfer and orbital overlap. In this first example, we highlight the subtle interplay between site potential and near neighbor interactions at controlling structure in metal-rich phosphides.

The recent synthesis and crystal structure determination of ZrNbP provide two unusual features:[37] (1) ZrNbP crystallizes in the Co_2Si structure type (oP12[*]), whereas Zr_2P (oC108) and Nb_2P (oP54) form other, quite complex structures; and (2) Zr and Nb are completely separated onto different crystallographic sites with no evidence for mixed site occupations nor of any variable composition, $Zr_{1\pm x}Nb_{1\mp x}P$. The miscibility of Zr and Nb is certainly manifested in their binary phase diagram, but does not seem to extend to this ternary compound. Furthermore, ZrNbP differs from ternary (Nb, Ta) sulfides,[38] in which there is only a partial segregation of Nb and Ta atoms onto inequivalent crystallographic sites. But ZrNbP is nonetheless similar to these ternary sulfides because they exist only for specific Ta:Nb ratios. Semi-empirical electronic structure calculations[39] were performed in our group in order to address the following questions: (1) what accounts for the complete segregation of Zr and Nb atoms in ZrNbP?, and (2) what controls the observed structure of ZrNbP with respect to viable alternative structures for the ternary MM′P phosphide system? As it turns out, both questions have the same answer, which relates to the nature of metal−metal bonding in this system. Moreover, the theoretical analysis predicted the structure for the new compound ZrMoP, which was subsequently confirmed by experiment. Therefore, the structure and existence of a new intermetallic compound could be predicted using crystal chemical principles and electronic structure calculations.

Figure 7. (Top) structure of ZrNbP and (bottom) structure of ZrMoP; black circles are Nb or Mo atoms, gray circles are Zr atoms, and white circles are P atoms; figures on the left illustrate metal−phosphorus contacts, figures on the right show metal−metal contacts

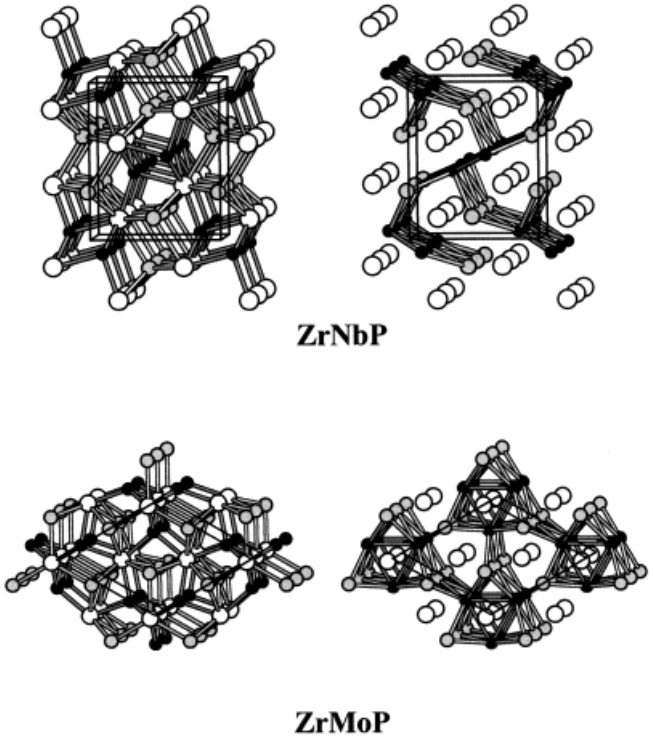

Figure 7 illustrates two projections of ZrNbP along the crystallographic b axis, one of which emphasizes the close metal−phosphorus contacts (d < 3.05 Å) while the other

[*] The Pearson symbol[32] describes for a given structure its Laue symmetry, lattice class, and number of atoms in the unit cell. oP12 means primitive orthorhombic with 12 atoms in the unit cell.

shows the metal−metal distances shorter than 3.30 Å. In ZrNbP, Nb is tetrahedrally coordinated and Zr is square pyramidally coordinated by P atoms. With respect to these coordination environments, there are two alternative structures common to many ABC intermetallics: (1) the Fe_2P-type and (2) the Cu_2Sb-type.[32][40] The Fe_2P structure type is also illustrated in Figure 7 to point out both the metal−phosphorus and metal−metal connectivities. In order to compare the total energies of the three structure types at valence electron counts around fourteen per formula unit, second moment scaling and the structural energy theorem were applied. Figure 8 illustrates these results as energy difference curves. Not only do these calculations reflect the stability of the observed structure for ZrNbP, but they also predict the structure of ZrMoP, if it exists, to be the Fe_2P-type. Direct synthesis and single crystal structural characterization of $Hf_{1.06}Mo_{0.94}P$ confirmed this prediction, and revealed the complete segregation of Hf and Mo, respectively, onto the square pyramidal and tetrahedral sites.[39] ZrMoP was also synthesized and characterized by X-ray powder diffraction.[39]

Figure 8. Energy difference curves vs. valence electron count for the Co_2Si-, Fe_2P-, and Cu_2Sb-structure types as possible models for the structure of ZrNbP; the energy of the Co_2Si-structure type is the reference energy ($\Delta E = 0$); the lowest ΔE curve for a given electron count represents the most stable structure among the three models; the electron counts for ZrNbP and ZrMoP are marked

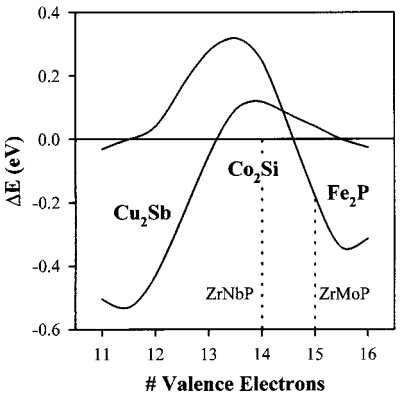

Why does the complete segregation of Zr and Nb in ZrNbP and of Hf and Mo in $Hf_{1.06}Mo_{0.94}P$ occur? The same electronic structure calculations[39] show that the observed, completely segregated sets of metal atoms give the lowest total valence electron energies over all other possible arrangements of metal atoms in ZrNbP and ZrMoP. From equation (8), this segregation provides the lowest site energies for these elements. In addition, analysis of the overlap populations[39][41] for the two shortest metal−metal contacts in each structure reveals that the *heteronuclear* Zr−Nb and Zr−Mo interactions are optimized, i.e., bonding and nonbonding orbitals are filled; antibonding orbitals are empty. At the corresponding Fermi levels, the homonuclear Nb−Nb interactions in ZrNbP are nonbonding whereas the Mo−Mo contacts in ZrMoP show significant antibonding overlap (see Figure 9). These theoretical results are well reflected in the observed bond lengths: the shortest heteronuclear metal−metal distances reflect the differences in atomic radii [d_{min} (Zr−Nb) = 3.014 Å in ZrNbP vs. d_{min} (Hf−Mo) = 2.915 Å in HfMoP], whereas the shortest homonuclear metal−metal distances demonstrate the nature of occupied electronic levels near the Fermi level [d_{min} (Nb−Nb) = 2.816 Å in ZrNbP vs. d_{min} (Mo−Mo) = 3.015 Å in HfMoP]. Thus, total segregation of Zr and Nb in ZrNbP or Hf and Mo in $Hf_{1.06}Mo_{0.94}P$ relies not only on the site energies in each structure, but also on the heteronuclear metal−metal interactions.

Figure 10 illustrates how the relationship between the site and bond energies arises. Phosphorus atoms create tetrahedral and square pyramidal ligand fields about the metals, which breaks the degeneracy of their valence *d* orbitals. According to electronegativities (see Figure 6) some of the metal valence electrons are transferred to phosphorus to form metal−phosphorus bonds. The electrons remaining in metal valence orbitals are utilized to form heteronuclear and homonuclear metal−metal bonds. Since the strength of orbital interactions is inversely proportional to the energy difference between the two isolated orbitals,[14] the strongest heteronuclear metal−metal interactions occur when the energy difference between occupied valence *d* orbitals of the

Figure 9. Overlap populations[17][41] for the shortest homonuclear and heteronuclear metal−metal bonds in ZrNbP (left) and ZrMoP (right); the dashed lines indicate calculated Fermi levels for 14 and 15 valence electrons per formula unit; positive values (bonding overlap) lie to the right and negative values (antibonding overlap) lie to the left; in ZrNbP, both Nb−Nb and Zr−Nb bonding is optimized; in ZrMoP, Zr−Mo bonding is optimized, but there is significant antibonding character for Mo−Mo bonding at the Fermi level

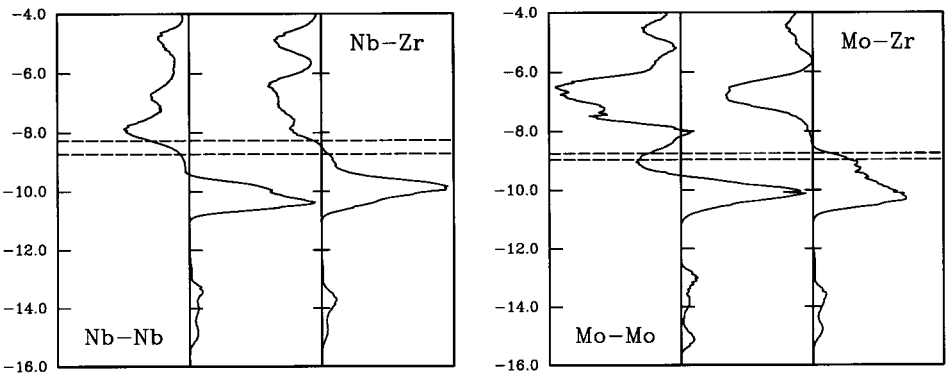

two different metals is smallest. In ZrNbP and ZrMoP this condition is met when Zr is in square pyramidal coordination and Nb or Mo are tetrahedrally coordinated by P: the difference in valence *d* orbital energies equals the free atomic orbital energy difference, Δ, plus the difference between the *d* orbital energy shifts from the π donor phosphorus ligands (expressed in units of e_π using the angular overlap model[2]). When the more electronegative Nb or Mo atoms are tetrahedrally coordinated, the resulting energy difference is less than when these elements are in the square pyramidal sites. In this manner, optimizing the site energy also minimizes the heteronuclear metal−metal bond energy.

Figure 10. Ligand field effects on the site preference problem in metal-rich ternary phosphides; in each section, the relative energies of the Zr and Nb 4*d* AOs are shown (Δ is energy difference between Nb and Zr 4*d* AOs); under the influence of either tetrahedral or square pyramidal ligand fields of phosphorus, these 4*d* orbitals are split and pushed up in energy by M−P σ* and π* interactions (e_π and e_π' are AOM parameters[2]); (left) $\Delta E = \Delta + 2e_\pi' - 2.7e_\pi$; (right) $\Delta E' = \Delta + 2.7e_\pi' - 2e_\pi$; $\Delta E < \Delta E'$

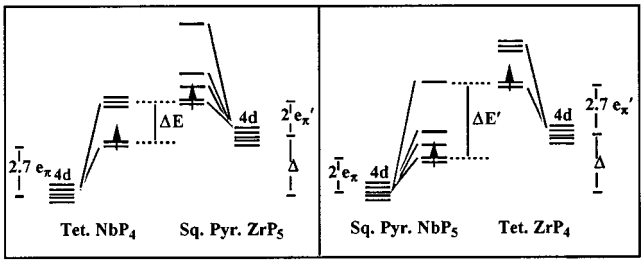

3. Coloring and Composition in Aluminides: Zintl Phases?

The question of chemical composition is closely linked to stable electronic configurations. For ionic and valence compounds (Zintl phases), the octet rule allows the chemist to "understand" chemical stability, since all bonding and nonbonding orbitals should be filled for "stable" chemical species.[42] When the electronegativity differences between elements in a compound are small, as in intermetallics, this rule becomes less well defined, and electronic structure calculations are necessary for a complete analysis. Nevertheless, the principle of bond order optimization by filling bonding and nonbonding orbitals is a compelling driving force for stable chemical compositions in a specific structure, i.e., equations (3) or (8).

Aluminides have been the focus of recent research towards an understanding of the transition from intermetallics to Zintl phases.[43] Post-transition elements form Hume-Rothery compounds[9] with *vec* < 2, while Zintl phases have networks of these elements with *vec* ≥ 4. Ternary aluminides involving an alkali or alkaline earth metal and an element from groups 11, 12, or 13 allow examination of compounds with *vec* values between two and four. A recent example of these efforts is $BaCu_5Al_8$,[44] which adopts the $NaZn_{13}$-type intermetallic structure. Further efforts have demonstrated that this structure occurs for compounds $ACu_{5\pm\varepsilon}Al_{8\mp\varepsilon}$, with A being Ba, Sr, La, or Eu and $\varepsilon \leq 1$.[45] The $NaZn_{13}$ structure type, shown in Figure 11, is a three-dimensional network of interconnected atom-centered (stuffed) icosahedra. Within the $[Cu_{5\pm\varepsilon}Al_{8\mp\varepsilon}]$ icosahedral substructure, there are two crystallographically inequivalent sites: (1) the center of each icosahedron, which is exclusively occupied by Cu; and (2) the surface of each icosahedron which is randomly decorated with $(4 \pm \varepsilon)$ Cu and $(8 \mp \varepsilon)$ Al atoms. Thorough synthetic and crystallographic investigations indicate that no ordering of Cu and Al on the icosahedra occurs even after months of annealing above 1000°C. Electronic structure calculations on various arrangements of Cu and Al in $BaCu_5Al_8$ demonstrate that bonding within the icosahedral framework is optimized (see Figure 11). Combinatorial methods indicate only ten unique ways of arranging four Cu and eight Al atoms in an icosahedron.[46][47] According to molecular orbital calculations, the lowest energy configurations of Cu and Al maximize the separations between Cu atoms. But, since there are six intericosahedral contacts per cluster, there is little energetic driving force for the ordering of Cu and Al. On the other hand, the overlap population curve in Figure 11 suggests that the stable compositions are influenced by the

Figure 11. (Top) structure of $BaCu_5Al_8$; shaded circles are Ba atoms, icosahedra correspond to the Cu-centered $[Cu_4Al_8]$ clusters which are tightly interconnected; (bottom) overlap populations for two types of bonds in the icosahedral network: (i) central Cu with surface atoms, and (ii) among difference surface atoms on the icosahedra; note that bonding orbitals are filled and antibonding orbitals are empty at the Fermi level for $BaCu_5Al_8$

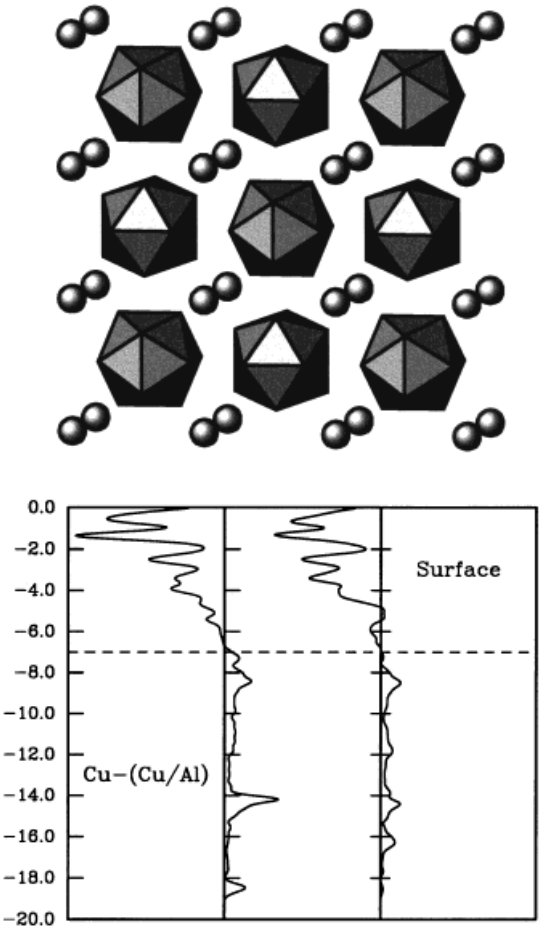

valence electron concentration and contribute to the narrow range of composition that has been observed.

Corresponding reactions with the more electronegative coinage metal, Au, rather than Cu produce a structure which is related to the $NaZn_{13}$-type, but the icosahedron is empty and there is an ordering of Au and Al atoms on the icosahedra (see Figure 12).[45] Both observations result from the repulsive Au−Au interactions that are present in this chemical environment: Au is the most electronegative component which attracts electrons from Al and increases the antibonding interaction between Au atoms. The arrangement of Au and Al corresponds to the lowest energy Au_4Al_8 icosahedron as calculated by molecular orbital methods.

Figure 12. Icosahedron found in $SrAu_{5+x}Al_{7-x}$; black circles are Au atoms, gray circles are a mixture of Au and Al atoms, white circles are Al atoms; the arrangement for the four black Au atoms corresponds to the lowest energy configuration of the icosahedron $[Au_4Al_8]$

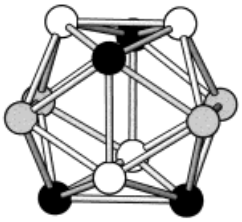

Further investigations with Au in this reducing environment produce new compounds[45][48][49] which allow an investigation of the chemistry and coloring problem involving the $BaAl_4$ structure, which is the most prolific intermetallic structure reported, known for more than 600 compounds.[50] This tetragonal structure contains two crystallographically distinct sets of aluminum atoms: one set forms planar square nets (Wyckoff site 4*e*) while the other set form dimers (Wyckoff site 4*f*) which link the square nets together to form a three-dimensional framework. There are numerous ternary variants of $BaAl_4$, in which the Al positions are occupied by two different elements in various ways (see Figure 13): (1) the $ThCr_2Si_2$-type, space group *I*4/*mmm*, with the different elements occupying the two inequivalent crystallographic sites; (2) the $CaBe_2Ge_2$-type, space group *P*4/*nmm*, in which the two elements alternate occupying the layers of square nets and the dimers so that only heteronuclear "Be−Ge" nearest neighbor contacts occur; and (3) the $BaNiSn_3$-type, space group *I*4*mm*, in which the Sn atoms form the square nets and the heteroatomic "Ni−Sn" pairs align in the same direction throughout the structure. The electronic structures of many compounds with these atomic arrangements have been extensively examined[51] and the results are summarized as follows: (1) for main group compounds, the structure is observed with 12−14 valence electrons per formula unit; (2) bonding within each dimer involves two-center two-electron σ bonds at 14 valence electrons, with an increasing π bonding character towards 12 valence electrons; and (3) optimum bonding between atoms on the 4*e* and 4*f* sites occurs at 12 valence electrons, and involves multi-center orbital interactions.

Figure 13. Three different colorings of $BaAl_4$ in ternary $LnAu_{1+x}Al_{3-x}$ intermetallics; black circles are Au atoms, dark gray circles (in center diagram only) are 50% Au/50% Al atoms, light gray circles are Al atoms, white circles are Ln atoms; (top) $LnAuAl_3$; (center) $LnAu_{1+x}Al_{3-x}$ ($0 < x \leq 0.5$); (bottom) $LnAu_2Al_2$

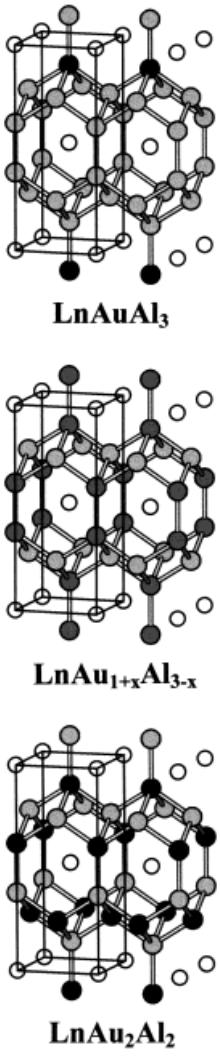

Recent investigations in ternary rare earth/gold/aluminum systems have shown interesting trends with respect to the "coloring" of Au and Al atoms in the covalent network of the $BaAl_4$ structure.[45][48] $LnAu_xAl_{4-x}$, $0.75 \leq x \leq 2$, have been reported for Ln ranging from La to Tb. When $x \geq 1.5$, the $CaBe_2Ge_2$ structure type occurs. For $x < 1.5$, i.e., higher Al concentrations, Au and Al partially disorder to give the $ThCr_2Si_2$-type until the composition $LnAuAl_3$, which shows both the ordered $BaNiSn_3$ and disordered $CeCuAl_3$ structure types. At $x = 0.75$, Au and Al are disordered on the 4*f* site, and show features of the $ThCr_2Si_2$ structure. Therefore, an interesting trend in coloring phenomenon occurs as the composition varies in $LnAu_xAl_{4-x}$ and for which the structural topology remains unchanged. Using equation (8) for these systems, the site energy is minimized when the most electronegative component occupies the 4*e* site, which is the place where Au replaces Al at low Au concentration ($x \leq 1$). As the Au

concentration increases, repulsive Au−Au interactions "force" Au atoms to occupy the square net positions 4*d*, until the maximum Au composition $LnAu_2Al_2$ is achieved. If the Au composition were to extend beyond this compound, Au−Au contacts would become necessary. Furthermore, the lowest possible Au concentration is $LnAu_{0.5}Al_{3.5}$ in order to maintain a maximum *vec* of fourteen electrons. When $x < 1$, entropic factors favor the body-centered tetragonal $BaAl_4$-type over the primitive tetragonal $BaNiSn_3$-type with no long range preference for the ordering of Au and Al in the dimers, which is observed for $EuAu_{0.75}Al_{3.25}$[45] Recent experiments have also shown that ordered vacancies enter the Au−Al framework as *vec* approaches fourteen electrons to give $Ln_3Au_2Al_9$ (Ln = Sm, Gd, Tb, Dy, and Yb).[45][49][52]

4. Coloring: Structure and Composition in Main Group Laves Phases

In the previous two sections, we have discussed how the coloring problem is tied to either structure or composition in intermetallic compounds. In general, however, these three aspects are closely interrelated, and are often difficult to separate and investigate systematically. An example of this problem occurs in the Ca−Li−Al ternary phase diagram along the line $CaLi_xAl_{2-x}$, which can be reformulated as $(CaLi_2)_y/(CaAl_2)_{1-y}$, $x = 2y$.[53] $CaLi_2$ and $CaAl_2$ form different Laves phase structures:[54] $CaLi_2$ adopts the hexagonal $MgZn_2$-type; and $CaAl_2$ forms the cubic $MgCu_2$-type. There exist many investigations concerning the influence of *vec* on the structures of Laves phases, but this study was the first which pointed out partial site preferences taking place in the framework of the majority component. Figure 14 illustrates how the volumes of the observed phases vary with Li content. When compared to a linear interpolation between the two binary compounds, there is a considerable volume reduction for the ternaries which strongly suggests covalent bonding within the aluminum framework, as found in Zintl phases. As x increases from zero in $CaLi_xAl_{2-x}$, the cubic $MgCu_2$-type structure changes to the hexagonal $MgNi_2$-type structure and then to the $MgZn_2$-type structure. Furthermore, stable compounds occur in $CaLi_xAl_{2-x}$ only for $x < 1$; when synthesis is attempted for phases with $x \geq 1$, disproportionation into $CaLi_2$ and $CaLi_yAl_{2-y}$, $y < 1$, occurs.

With respect to the coloring problem in Laves phases, the cubic $MgCu_2$-type structure has just one kind of majority site, whereas the hexagonal $MgNi_2$ and $MgZn_2$ types have three and two kinds of majority sites, respectively, which lead to potential site preferences. Li and Al show no site preferences in the hexagonal $MgNi_2$-type compounds, e.g., $CaLi_{0.33}Al_{1.67}$, and partial site preferences in the $MgZn_2$-type examples, e.g., $CaLi_{0.88}Al_{1.12}$. In this last compound, one of the majority sites (the kagomé nets; Wyckoff site 6*h*) is 50% Li and 50% Al, while the other crystallographic site (Wyckoff site 2*a*) attracts 75% Al and 25% Li. The reasons for these two coloring patterns stem from both the site energies as well as the driving force for Al in this reducing environment to establish an octet by forming Al−Al bonds.

Figure 14. $CaLi_xAl_{2-x}$ phases; (top) variation in volume per formula unit as the Li content varies from 0% to 100%; the dashed line connecting the two endpoints ($CaAl_2$ and $CaLi_2$) represents Zen's law for a linear variation with composition; the vertical dashed lines separate regions of the types of Laves phase structure observed for the experimental points; (bottom) trend in charges of the majority elements (Li_xAl_{2-x}) for the hexagonal $MgZn_2$-structure type as the number of valence electrons changes; the dashed line shows the maximum number of valence electrons allowed for this structure; the 2*a* site gains electrons, the 6*h* site loses electrons: thus, the more electronegative element would be attracted to the 2*a* site

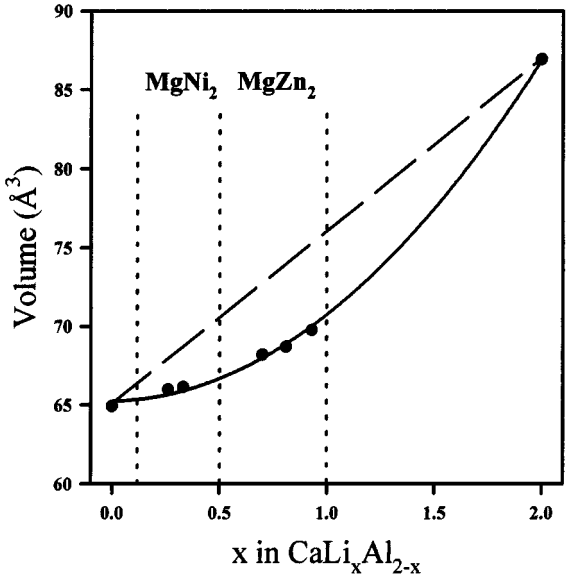

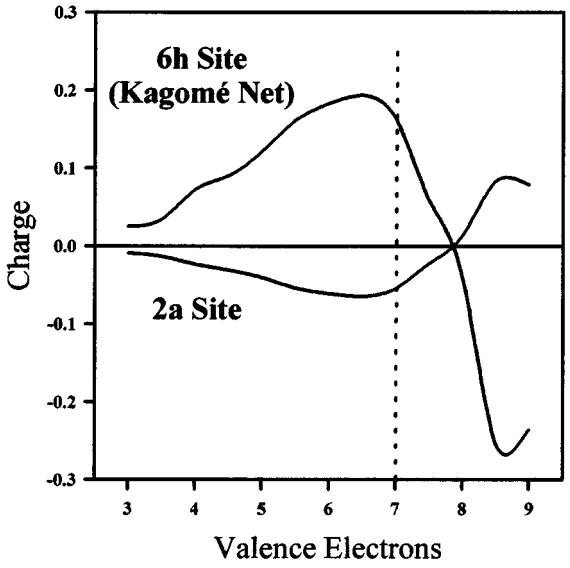

For the series of observed $CaLi_xAl_{2-x}$ compounds, both semiempirical and density functional theory show that Ca donates just one valence electron to the $[Li_xAl_{2-x}]$ framework. Figure 14 illustrates the deviations from the average Mulliken population for the two majority sites in the hexagonal $MgZn_2$-type structure as a function of valence electron count. Notice that the largest difference in atomic population occurs for six electrons per formula unit

("CaLiAl"), whereas the difference is nearly zero between seven and eight electrons. Thus, $CaAl_2$ (8 electrons) and $CaLi_{0.33}Al_{1.67}$ (7.33 electrons) adopt, respectively, the $MgCu_2$-type and the $MgNi_2$-type structures with no site preferences. On the other hand, $CaLi_{0.88}Al_{1.12}$ (6.25 electrons) do show segregation in agreement with the Mulliken population analysis. However, with respect to minimizing the bond energy component of the total orbital energy from equation (8), a completely random arrangement of Li and Al would be expected. If the Zintl-Klemm formalism is applied to Al in $CaLi_{0.88}Al_{1.12}$ with complete segregation of Li and Al into the two crystallographic sites as far as allowed by the composition, the Ca atoms would donate 1.2 electrons to the $[Li_{0.88}Al_{1.12}]$ framework, which opposes the conclusions from theoretical calculations. Table 1 summarizes three different scenarios for the arrangement of Li and Al atoms in $CaLi_{0.88}Al_{1.12}$: (1) minimum site energy, (2) minimum Al−Al bond energy, and (3) the observed configuration. These results demonstrate that the structure and the partial segregation of Li and Al arise from the synergistic interplay of both the site energy and bond energy terms in the total orbital energy. In addition, the observed structure optimizes the Ca−Ca orbital interactions, as has been shown by calculating pair potentials in $CaAl_2$.[55] In $CaLi_{0.33}Al_{1.67}$, both the site energy and bond energy terms allow for a completely random arrangement of Li and Al throughout the structure.

5. Coloring and Property Effects in Metal-Rich Tellurides

The cases discussed thus far demonstrate minor changes in physical or chemical properties as a function of atomic coloring. This is due primarily to the fact that either the electronic configurations are all closed shell (as in Nb_3SI_7), or the valence electron concentrations are sufficiently low (less than four per atom) as to preclude any significant change in electronic properties. In order to investigate effects of atomic coloring on conductivity properties, focus must be directed towards compounds involving the post-transition elements, whose structures lie close to the border between Zintl phases (valence compounds) and typical intermetallics (Hume−Rothery phases, for example). A particularly interesting set of examples involves the substitution of Sn atoms for Tl atoms in the low temperature superconductor Tl_5Te_3.

Tl_5Te_3 adopts a variation of the tetragonal Cr_5B_3-structure type with a smaller than typical *c*/*a* ratio for these compounds, which leads to a three-dimensional network of vertex-sharing octahedra, $^3_\infty[TlTe_{6/2}]$, stuffed with Tl atoms over each face of the octahedron, i.e., $[TlTe_{6/2}]Tl_{8/2} \triangleq Tl_5Te_3$ (see Figure 15).[56] Tl_5Te_3 has a superconducting transition at 2.2 K,[57] which according to a combination of band structure and lattice energy calculations,[58] can arise from an electronic instability in the electronic band structure that is frustrated by strong short-range repulsive forces which retard any structural distortion. Using simple electron counting, the octahedrally coordinated Tl atoms can be formulated as Tl^{2+}, which is unstable towards disproportionation into Tl^{+1} and Tl^{3+}.[20]

Figure 15. The structure of Tl_5Te_3 and its ternary derivatives; white circles are Te atoms, black circles are Tl atoms; Te octahedra are also illustrated; there is a Tl atom at the center of each octahedron

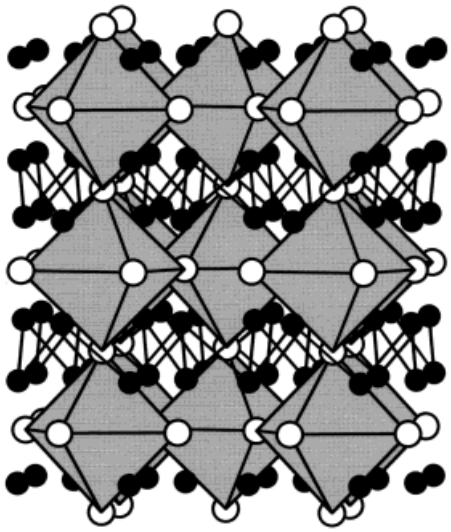

Böttcher and coworkers have recently synthesized ternary derivatives of Tl_5Te_3.[59] In particular, $SnTl_4Te_3$ was prepared and shown to be metallic. From crystallographic data, the Sn atoms occupy both Tl sites in the parent structure. Replacing a "Tl^{2+}" with a Sn^{2+} is a plausible chemical

Table 1. Analysis of various coloring models for the $MgZn_2$-type Laves phase $CaLi_{0.88}Al_{1.12}$ with respect to the Zintl-Klemm formalism; the $[Li_{0.88}Al_{1.12}]$ network is described by two crystallographic sites in the space group $P6_3/mmc$: the 2*a* and the 6*h* sites

Coloring Model		− 2*a* Site − Site Occ.	CN by Al[a]	Charge[b]	− 6*h* Site − Site Occ.	CN by Al[a]	Charge[b]	Role of Ca: Electrons, Bond Order
Minimum Site Energy	Al:	100.00%	2.500	−2.500	41.67%	3.667	−1.333	Ca donates 1.21 electrons;
	Li:	0.00%		+1.000	58.33%		+1.000	Ca−Ca Bond Order ca. 0.6
Minimum Bond Energy	Al:	56.25%	3.375	−1.625	56.25%	3.375	−1.625	Ca donates 0.95 electron;
	Li:	43.75%		+1.000	43.75%		+1.000	Ca−Ca Bond Order ca. 0.9
Observed Arrangement	Al:	75.00%	3.000	−2.000	50.00%	3.500	−1.500	Ca donates 1 electron;
	Li:	25.00%		+1.000	50.00%		+1.000	Ca−Ca Bond Order ca. 1.0

[a] CN = coordination number; it represents the average number of Al nearest neighbors. − [b] Charge for Al is based on the 8 − *N*rule; it equals 3 − (8 − CN) = CN − 5. The charge for Li is chosen to be +1 as the most electropositive element in this compound.

substitution, and with an increase the valence electron concentration to a closed subshell configuration, semiconducting behavior would be expected. Indeed, band calculations with Sn completely replacing the octahedrally coordinated Tl atoms produces an energy gap at the Fermi level (Model A: see Figure 16). A combination of electronic band structure and lattice energy calculations reveal that whereas covalent interactions prefer Sn atoms to substitute at the octahedral sites, ionic interactions would rather place Sn atoms at the other Tl sites.[58] When such a substitution mode takes place, $SnTl_4Te_3$ retains its metallic character, but yields a smaller density of states at the Fermi level (Model B: see Figure 16). Therefore, where the substitution for Tl takes place has a dramatic effect on the expected physical properties of the derivative compounds.

Figure 16. Densities of states for two models of Sn atom coloring in $SnTl_4Te_3$; (left) Model A: all Sn atoms occupy the octahedral sites shown as polyhedra in Figure 15; (right) Model B: all Sn atoms occupy the other Tl sites shown as black circles in Figure 15; note that the Fermi level occurs in an energy gap for Model A, but there is no gap in Model B

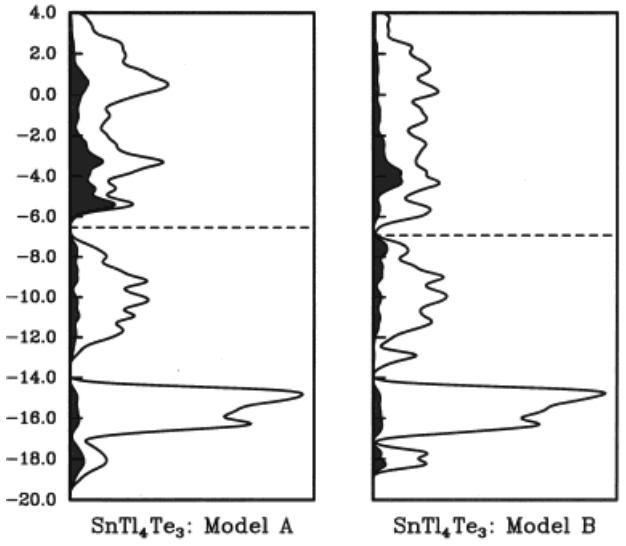

Summary, Implications, and Future Directions

The coloring problem has powerful ramifications in chemistry. Electronic structure theory provides a theoretical underpinning for its effects, and also allows a simple chemical understanding of the phenomenon. However, can theory really assist the synthetic chemist with this problem? One important goal of synthetic chemists is to prepare new materials, which is often motivated by trying to optimize certain chemical or physical properties, e.g., catalytic activity, thermoelectric behavior, or magnetism to name a few. For the solid state chemist, these efforts are largely Edisonian in nature. Of course, the discovery of some physical property in one example tends to attract attention to the particular structure type in question: for example, superconductivity in cuprates. A working knowledge of the coloring problem, which includes both an imagination for possible new structures as well as an analysis based upon existing structures, will greatly assist the synthetic solid state chemist as the search for new, exciting, and probably more complex materials continues. Complexity can be simply moving from binary to ternary to quaternary systems, where the number of possible new materials increases exponentially.

How atoms arrange themselves in extended solid state structures depends on the number of valence electrons and the differences in electrochemical potentials, which are related to electronegativity, size, and the types of valence electronic structure the atoms bring to the compound. This review attempted to demonstrate that not only is structure a concern, but also the decoration pattern once a network of atoms is in place. Structure-composition-property interrelationships can then be studied by a careful application of experiment and theory − in most cases involving intermetallic compounds, theory is essential in order to develop a description of the electronic structure that harks to the classical chemical ideas for valence compounds. A partitioning of the total electronic energy into a site energy and a bond energy creates two components to the coloring problem. Through the examples presented in this review, i.e., Nb_3SI_7, ZrNbP and ZrMoP, $BaCu_5Al_8$ and $SrAu_6Al_6$, $LnAu_xAl_{4-x}$, $CaLi_xAl_{2-x}$, and $Sn_xTl_{5-x}Te_3$, analysis of both components is necessary to understand the complete structural details of these compounds and to ultimately relate their structures to their physical properties.

Where does the coloring problem take us now? A couple of examples may provide an indication: (1) utilize the Klemm pseudoelement approach[60] to create possible mixed anion matrices for transition metals in order to study electronic transitions, e.g., metal-semiconductor or metal-superconductor transitions, and (2) rely on structural experience in crystalline solids to develop models for systems which lack translational symmetry and yet are beginning to show interesting properties and applications with little fundamental understanding, i.e., quasicrystals and amorphous metals.[61] Our group is beginning to address these questions using the elegant ideas surrounding the coloring problem.

My group's efforts in this field have benefited by the financial support of the *Department of Energy*, the Donors of the *Petroleum Research Fund*, administered by the *American Chemical Society*, and the *National Science Foundation* (DMR-96-27161). The author is indebted to *Jun Cheng*, *Chi-Shen Lee*, *Jianhua Lin*, *Karen Nordell*, and *Mark Smith* for significant contributions to some of the work presented in this microreview, and to *Carla Holbrook* for some of the figures.

☆ Dedicated to the memory of Professor *Jeremy K. Burdett*, who was a brilliant scientist and a superb mentor.

[1] H.-D. Hardt, *Die periodischen Eigenschaften der chemischen Elemente*, 2. Auflage, Georg Thieme Verlag, Stuttgart, **1987**, p. 126.
[2] J. K. Burdett, *Molecular Shapes*, Wiley Interscience, New York, **1980**.
[3] J. Donohue, *The Structure of the Elements*, Krieger, Malabar, Florida, **1982**.
[4] D. G. Pettifor, *Bonding and Structure of Molecules and Solids*, Oxford University Press, Oxford, **1995**.
[5] P. Pyykkö, *Adv. Quant. Chem.* **1978**, *11*, 353; P. Pyykkö, J. P. Desclaux, *Acc. Chem. Res.* **1979**, *12*, 276; P. Pyykkö, *Chem. Rev.* **1988**, *88*, 563.
[6] D. G. Pettifor, R. Podloucky, *Phys. Rev. Lett.* **1984**, *53*, 1080; J. K. Burdett, S. Lee, *J. Am. Chem. Soc.* **1985**, *107*, 3063; S. Lee,

Acc. Chem. Res. **1991**, *24*, 249; S. Lee, *J. Am. Chem. Soc.* **1991**, *113*, 101, 8611; L. Hoistad, S. Lee, *J. Am. Chem. Soc.* **1991**, *113*, 8216.
[7] T. L. Brennan, J. K. Burdett, *Inorg. Chem.* **1993**, *32*, 750.
[8] J. K. Burdett, S. Lee, T. J. McLarnan, *J. Am. Chem. Soc.* **1985**, *107*, 3083.
[9] W. Hume-Rothery, *J. Inst. Metals* **1926**, *35*, 295.
[10] D. Barnette, *Map Coloring, Polyhedra, and the Four-Color Problem*, The Mathematical Association of America, USA, **1983**.
[11] H. S. M. Coxeter, *Introduction to Geometry*, Wiley, New York, **1969**.
[12] F. Harary, *Graph Theory*, Addison-Wesley Publishing Co., Reading, MA, USA, **1972**.
[13] J. K. Burdett, E. Canadell, T. Hughbanks, *J. Am. Chem. Soc.* **1986**, *108*, 3971.
[14] T. A. Albright, J. K. Burdett,, M.-H. Whangbo, *Orbital Interactions in Chemistry*, Wiley-Interscience, New York, **1985**.
[15] S_4N_4: M. L. de Lucia, P. Coppens, *Inorg. Chem.* **1978**, *17*, 2336; As_4S_4: D. J. E. Mullen, W. Nowacki, *Z. Kristallogr. Kristallgeom. Kristallphys. Kristallochem.* **1972**, *136*, 48.
[16] B. M. Gimarc, *J. Am. Chem. Soc.* **1983**, *105*, 1979.
[17] R. Hoffmann, *Solids and Surfaces: A Chemist's View of Bonding in Extended Structures*, VCH Publishers, New York, **1988**; J. K. Burdett, *Prog. Solid State Chem.* **1984**, *15*, 173; R. S. Mulliken, *J. Chem. Phys.* **1955**, *23*, 1833, 2343.
[18] C. A. Coulson, *Proc. Roy. Soc. London, Ser. A* **1939**, *139*, 413.
[19] I. N. Levine, *Quantum Chemistry*, 2nd ed., Allyn, Bacon, Inc., Boston, **1974**, pp. 421-450.
[20] N. N. Greenwood, A. Earnshaw, *Chemistry of the Elements*, Pergamon Press, Oxford, **1984**.
[21] G. C. Pimentel, *J.Chem. Phys.* **1951**, *19*, 446; R. J. Hach, R. E. Rundle, *J. Am. Chem. Soc.* **1951**, *73*, 4321.
[22] R. Hoffmann, W. N. Lipscomb, *J. Chem. Phys.* **1962**, *36*, 2179, 3489; R. Hoffmann, *J. Chem. Phys.* **1963**, *39*, 1397; J. H. Ammeter, H.-B. Bürgi, J. C. Thibeault, R. Hoffmann, *J. Am. Chem. Soc.* **1978**, *100*, 3686.
[23] A. P. Sutton, *Electronic Structure of Materials*, Clarendon Press, Oxford, **1994**.
[24] R. Haydock, V. Heine, M. Kelly, *J. Phys. C* **1972**, *5*, 2845; V. Heine, R. Haydock, D. Bullett, M. Kelly, *Solid State Physics* **1980**, *35*, 1; D. G. Pettifor, D. L. Weaire (Eds.), *The Recursion Method and its Applications*, Springer-Verlag, Heidelberg, **1985**.
[25] K_2SnTe_5: B. Eisenmann, H. Schwerer, H. Schäfer, *Mater. Res. Bull.* **1983**, *18*, 383; Tl_2SnTe_5: V. Agafonov, P. Legendre, N. Rodier, J. M. Cense, E. Dichi, G. Kra, *Acta Crystallogr., Sect. C* **1991**, *47*, 850.
[26] J. B. Goodenough, A. L. Loeb, *Phys. Rev.* **1955**, *98*, 391.
[27] J. K. Burdett, T. J. McLarnan, *J. Solid State Chem.* **1984**, *53*, 382; J. K. Burdett, *Chemical Bonding in Solids*, Oxford University Press, Oxford, **1995**.
[28] E. Zintl, W. Dullenkopf, *Z. Phys. Chem.* **1932**, *B16*, 195.
[29] G. J. Miller, *J. Alloys Compd.* **1995**, *229*, 93; G. J. Miller, *J. Alloys Compd.* **1995**, *217*, 5.
[30] H. Schäfer, H. G. von Schnering, *Angew. Chem.* **1964**, *76*, 833.
[31] A. Simon, H. G. von Schnering, *J. Less-Common Met.* **1966**, *11*, 31.
[32] W. B. Pearson, *The Crystal Chemistry and Physics of Metals and Alloys*, Wiley, New York, **1972**.
[33] F. Seitz, *The Modern Theory of Solids*, Dover Publications, Inc., New York, **1987**, pp. 76−98.
[34] G. J. Miller, J. Lin, *Angew. Chem.* **1994**, *106*, 357; *Angew. Chem. Int. Ed. Engl.* **1994**, *33*, 334; P. Schmitz, University of Freiberg, private communication, **1997**.
[35] C.-S. Lee, M.Sc. Thesis, *The Site Preference Study of Trinuclear Niobium Compounds $Nb_3(S_xI_{1-x})I_7$ ($x = 0.0-1.0$)*, Iowa State University, **1997**; G. J. Miller, J. Lin, M. D. Smith, C. S. Lee, manuscript in preparation.
[36] V. Heine, I. J. Robertson, M. C. Payne in *Bonding and Structure of Solids*, The Royal Society, London, **1991**, p. 1.
[37] G. Marking, H. F. Franzen, *J. Alloys Compd.* **1994**, *204*, L16.
[38] B. Harbrecht, H. F. Franzen, *Z. Anorg. Allg. Chem.* **1987**, *551*, 74; B. Harbrecht, *Z. Kristallogr.* **1988**, *182*, 118; B. Harbrecht, H. F. Franzen, *Z. Kristallogr.* **1989**, *186*, 119; X. Yao, H. F. Franzen, *J. Less-Common Met.* **1990**, *161*, L37; X. Yao, H. F. Franzen, *J. Solid State Chem.* **1990**, *86*, 88; X. Yao, H. F. Franzen, *Z. Anorg. Allg. Chem.* **1991**, *598*, 353; X. Yao, H. F. Franzen, *J. Am. Chem. Soc.* **1991**, *113*, 1426; X. Yao, G. J. Miller, H. F. Franzen, *J. Alloys Compd.* **1992**, *183*, 7; H. F. Franzen, M. Köckerling, *Prog. Solid State Chem.* **1995**, *23*, 265.
[39] G. J. Miller, J. Cheng, *Inorg. Chem.* **1995**, *34*, 2962.
[40] B. G. Hyde, S. Andersson, *Inorganic Crystal Structures*, Wiley Interscience, New York, **1989**.
[41] T. Hughbanks, R. Hoffmann, *J. Am. Chem. Soc.* **1983**, *105*, 3528; S. Wijeyesekera, R. Hoffmann, *Organometallics* **1984**, *3*, 949.
[42] G. J. Miller in *Chemistry, Structure, and Bonding of Zintl Phases and Ions* (Ed.: S. M. Kauzlarich), VCH Publishers, Inc., New York, **1996**, p. 1.
[43] R. Nesper, *Angew. Chem.* **1991**, *103*, 805; *Angew. Chem. Int. Ed. Engl.* **1991**, *30*, 789; U. Häussermann, S. Wengert, P. Hofmann, A. Savin, O. Jepsen, R. Nesper, *Angew. Chem.* **1994**, *106*, 2147; *Angew. Chem. Int. Ed. Engl.* **1994**, *33*, 2069; U. Häussermann, S. Wengert, R. Nesper, *Angew. Chem.* **1994**, *106*, 2150; *Angew. Chem. Int. Ed. Engl.* **1994**, *33*, 2073; U. Häussermann, M. Wörle, R. Nesper, *J. Am. Chem. Soc.* **1996**, *118*, 11789.
[44] K. J. Nordell, G. J. Miller, *Croat. Chim. Acta* **1995**, *68*, 825.
[45] K. J. Nordell, Ph.D. Thesis, *Exploring Aluminum-Rich Intermetallics with Experiment and Theory*, Iowa State University, **1997**.
[46] T. J. McLarnan, P. B. Moore in *Structure and Bonding in Solids*, vol. II (Eds.: M. O′Keeffe, A. Navrotsky), Academic Press, New York, **1981**.
[47] B. K. Teo, H. Zhang, Y. Kean, H. Dang, X. Shi, *J. Chem. Phys.* **1993**, *99*, 2929.
[48] F. Hulliger, H.-U. Nissen, R. Wessicken, *J. Alloys Compd.* **1994**, *206*, 263; F. Hulliger, *J. Alloys Compd.* **1995**, *218*, 255.
[49] For related gallides, see also: Yu. Grin, M. Ellner, K.Hiebl, P. Rogl, O. M. Sichevich, O. M. Myakush, *J. Alloys Compd.* **1994**, *205*, 285.
[50] P. Villars, L. D. Calvert, *Pearson's Handbook of Crystallographic Data for Intermetallic Phases*, 2nd ed., ASM, Materials Park, OH, **1991**.
[51] C. Zheng, R. Hoffmann, *Z. Naturforsch.* **1986**, *41B*, 292; J. K. Burdett, G. J. Miller, *Chem. Mater.* **1989**, *2*, 12; C. Zheng, *J. Am. Chem. Soc.* **1993**, *115*, 1047.
[52] K. J. Nordell, G. J. Miller, *Angew. Chem.* **1997**, *109*, 2098; *Angew. Chem. Int. Ed. Engl.* **1997**, *36*, 2008.
[53] R. Nesper, G. J. Miller, *J. Alloys Compd.* **1993**, *197*, 109.
[54] C. Barrett, T. B. Massalski, *Structure of Metals*, 3rd ed., Pergamon Press, Oxford, **1980**.
[55] J. Hafner, *From Hamiltonians to Phase Diagrams*, Springer-Verlag, Berlin, **1987**, p. 58.
[56] I. Schewe, P. Böttcher, H. G. von Schnering, *Z. Kristallogr.* **1989**, *188*, 287.
[57] A. Judoakis, C. R. Kannewurf, *J. Appl. Phys.* **1968**, *39*, 3003.
[58] K. J. Nordell, G. J. Miller, *J. Alloys Compd.* **1996**, *241*, 51.
[59] S. Bradtmöller, P. Böttcher, *Z. Anorg. Allg. Chem.* **1993**, *619*, 1155; S. Bradtmöller, P. Böttcher, *Z. Kristallogr.* **1994**, *209*, 75; S. Bradtmöller, P. Böttcher, *Z. Kristallogr.* **1994**, *209*, 97; S. Bradtmöller, Ph.D. Thesis, *Ternäre Metallreiche Chalkogenide: Synthese, Strukturen und Eigenschaften*, University of Düsseldorf, **1995**; T. Doert, Ph.D. Thesis, *Chalkogenide mit In_5Bi_3-Typ-Struktur*, University of Düsseldorf, **1994**.
[60] W. Klemm, *Proc. Chem. Soc., London* **1959**, 329; W. Klemm, *Trab. Reun. Int. React. Solidos, 3rd* **1956**, *1*, 447.
[61] A. I. Goldman, K. F. Kelton, *Rev. Mod. Phys.* **1993**, *65*, 213.

[97231]